M. GÓMEZ, S. F. MEDINA

"Promotion of Intragranular Nucleation of Ferrite in V-Microalloyed Steels"

Steel Research International,
Volume Extra, 2012, Pages 751-754
ISSN 1611-3683

Promotion of Intragranular Nucleation of Ferrite in V-Microalloyed Steels

Manuel Gómez[1)], **Sebastián F. Medina**[1)]

[1)] National Center for Metallurgical Research (CENIM-CSIC), Av. Gregorio del Amo 8; 28040-Madrid, Spain, mgomez@cenim.csic.es.

Abstract. The intragranular nucleation of ferrite was studied in three low-carbon microalloyed steels. Recrystallization-Precipitation-Time-Temperature (RPTT) diagrams were determined by means of isothermal double-deformation hot torsion tests. Once the diagrams were drawn, several tests were carried out where the samples suffered a single deformation and were cooled after a variable holding time at a characteristic temperature such as the precipitation nose temperature. Ferrite grain size was measured in these samples and the strengthening of austenite was measured by taking into account the unrecrystallized fraction of austenite before phase transformation. In this way, the relationship existing between precipitation state, fraction of austenite recrystallization and ferrite grain size was studied. It was found that V precipitates are more appropriate to promote intragranular nucleation than Nb precipitates. An increase in C, N and V contents promotes a precipitation state which seems to be more suitable for the intragranular nucleation to occur. The nucleation of very fine ferrite grains on V particles was assessed in another set of hot rolling simulation torsion tests carried under continuous-cooling conditions.

Keywords: microalloyed steel, precipitation, intragranular nucleation, ferrite grain refinement.

1. INTRODUCTION

The intragranular nucleation of ferrite in recrystallized or deformed austenite has become one of the most recent subjects of study in steels, with the aim of increasing the possibilities for several types of precipitates or inclusions to become nucleation sites [1,2]. In this way, in addition to the sites known as classic sources of heterogeneous nucleation of ferrite, such as grain boundaries and dislocations, the precipitated particles would represent a third way of contributing to refining the ferrite grain.

Some authors have studied the intragranular nucleation of idiomorphic and acicular ferrite on incoherent complex precipitates formed by MnS inclusions and V(C,N) precipitates [3-6]. Others have studied the intragranular nucleation of acicular ferrite on Ti_2O_3 particles and on mixed inclusions of MnS-CuS [7,8]. In general, these particles have proven to be efficient as nucleation sites for ferrite, and attention has been drawn to the important role played by MnS inclusions, even when they seem to be associated to Ti_2O_3 particles [9]. Several reasons have been proposed to justify the efficiency of these particles. On the one hand, the formation of MnS causes a local Mn impoverishment that favours the nucleation of ferrite. On the other hand, VC or VN has lower interfacial energy than ferrite but a relatively higher interfacial energy than austenite for the $(001)_{V(C,N)}$ boundary compared with MnS. These advantages of VC and VN over MnS in the balance of interphase boundary energy presumably promote the intragranular ferrite transformation for complex precipitates [10].

2. EXPERIMENTAL PROCEDURE

In this work, three low carbon microalloyed steels were studied. As shown in table 1, steel V1 and N1 had similar compositions and were respectively microalloyed with vanadium and niobium. Steel V2 was also a V-microalloyed steel but it had higher amounts of C and N.

Torsion specimens were prepared with a gauge length of 50 mm and diameter of 6 mm. Before torsion deformation, the samples were reheated for 10 min at a temperature above the solubility temperature of nitrides, carbides or carbonitrides, in order to put into solution the microalloying precipitates. Table 2 shows the solubility temperatures for the steels studied [11] and table 3 shows the austenite grain sizes measured after reheating. The recrystallized fraction was determined using the “back extrapolation” method [12] at different testing temperatures (between 850 ºC and 1100ºC), at equivalent strains of 0.20 and 0.35 and at a constant strain rate of 3.63 s^{-1}. With the aim of revealing the possible intragranular ferrite nucleation on V-precipitates, a further microscopy study, using a Jeol JSM 6500F scanning electron microscope equipped with a field emission gun (FEG-SEM), was carried out.

Table 1. Chemical composition of the studied steels (mass%).

Steel	C	Mn	Si	Al	S	V	Nb	N
V1	0.09	1.51	0.32	0.017	0.005	0.053	0.004	0.0052
N1	0.09	1.51	0.31	0.017	0.005	0.004	0.037	0.0040
V2	0.165	1.56	0.53	0.014	0.001	0.170	0	0.0160

Table 2. Solubility temperatures of the precipitates, according to Turkdogan’s solubility products [11].

Steel	Solubility Temperature, Ts (ºC)				
	$VC_{0.75}$	VN	$NbC_{0.87}$	NbN	$NbC_{0.7}N_{0.2}$
V1	737	926	--	--	--
N1	--	--	1090	1059	1124
V2	857	1146			

Table 3. Austenite grain sizes measured after reheating.

Steel	Reheat.temp.(x 10 min) ºC	Austenite grain size μm
V1	1100	67
N1	1200	95
V2	1230	80

3. RESULTS

3.1. Double deformation isothermal tests

For each steel and deformation used, the recrystallized fraction was drawn against time for each testing temperature (figure 1). It can be observed that some curves display a plateau caused by the formation of precipitates which momentarily block the progress of recrystallization. The start and finish of the plateau are identified approximately with the start and finish of induced precipitation. The curves corresponding to temperatures above those showing plateaus have the sigmoidal shape of Avrami’s law.

Besides, in the curves that show a plateau, the latter is not unlimited, i.e. precipitation does not permanently inhibit recrystallization, which finally progresses again until it is complete, following a graphic plot similar to that recorded before the formation of the plateau [13].

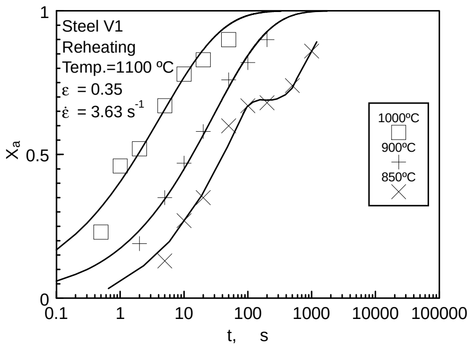

Figure 1. Variation in the recystallized fraction X_a with the time t for steel V1 and strain of 0.20.

Recrystallized fraction curves were used to plot recrystallization-precipitation-time-temperature (RPTT) diagrams as that shown in figure 2. The points that define the start and the end of the plateau were taken to plot the precipitation start (Ps) and finish (Pf) curves, respectively. The temperatures and times corresponding to different recrystallized fractions were also deduced from recrystallized fraction curves. The recrystallized fraction does not vary between the Ps and Pf curves and is represented by a horizontal line. Once the Pf curve is reached, the lines of each recrystallized fraction descend, meaning that as the temperature drops, more time is necessary to obtain a certain recrystallized fraction after straining. The most important magnitudes that can be deduced from a RPTT diagram are the minimum incubation time for precipitation, the minimum time for precipitation to finish, the curve nose temperature, the time that precipitation lasts, and finally the static recrystallization critical temperature (SRCT) [13].

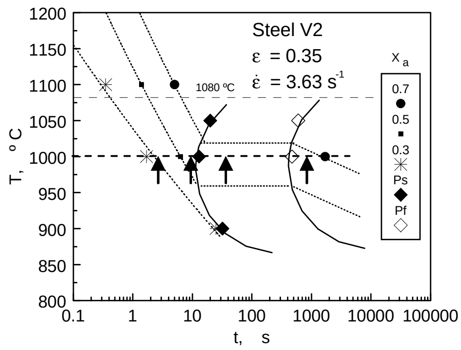

Figure 2. RPTT diagram of steel V2. The arrows indicate the post-deformation holding times before cooling.

3.2. Ferrite grain size and intragranular nucleation on isothermal tests

With the aim of studying the intragranular nucleation of ferrite by heterogeneous nucleation on the precipitates, specimens of the studied steels were deformed and held for a certain time, in accordance with the RPTT diagrams. After the holding time, the specimens were cooled with argon at a cooling rate (800-500 ºC) of approximately 3.5 K/s. The deformation conditions (strain, temperature, holding time) were selected in such a way as to approximately coincide with the curve nose temperature and with the precipitation start and finish times, previously applying the strain in accordance with the RPTT diagrams. For example, the arrows in fig. 2 show the post-deformation isothermal holding times for the case shown.

The metallographic study allowed the ferrite grain sizes to be measured by applying the linear intersection method on microstructures as that shown in figure 3. The ferrite grain size was measured for deformation conditions corresponding to points situated before, on and after the plateau. It should be noted that for deformation conditions corresponding to points on the plateau, the only variable that changes from one precipitation time to another longer time is the precipitation state (volume fraction and size of the particles), while the recrystallized fraction and the density of dislocations do not vary. Out of the plateaus, the recrystallized fraction would vary, as would the density of dislocations, which are important nucleation sites for ferrite.

Figure 3. Microstructure of steel N1 after the following treatment: reheating at 1200ºCx10 min, deformation at 975 ºC (ε = 0.20), holding time = 1000 s, argon cooling.

Figure 4 shows the evolution of ferrite grain size as a function of post-deformation holding time. As a first approach, it can be seen that Nb-steel N1 present smaller grain sizes than V-steel V1, despite the coarser initial austenite grain size shown in table 3. However, grain size is roughly constant for steel N1, whereas it presents a certain drop with time for steel V1, especially for ε = 0.20. On the other hand, steel V2 shows the finest grain size and a decrease with time can also be observed. The interpretation of this figure is complex, as several phenomena are occurring simultaneously during the holding time and subsequent cooling of the samples. After deformation, the austenite (with different initial grain size depending on the steel and the reheating conditions) starts to recrystallize. Recrystallization kinetics will depend on several aspects such as composition, austenite grain size, deformation conditions and holding temperature. Ferrite grain size obtained after cooling will depend on the volume fraction of recrystallized/deformed austenite, the grain size of recrystallized austenite and, if intragranular nucleation of ferrite occurs, also on the precipitation state.

In order to better analyze the possible occurrence of intragranular nucleation, figure 5 (which represents the ferrite grain size versus the recrystallized austenite fraction) was plotted. The evaluation of intragranular nucleation must be carried out in conditions where the only variable is the precipitation state, while the other variables like the recrystallized fraction (and therefore the dislocation density) and the average austenite grain size remain constant. For this reason, the corresponding precipitated volume percentage (Vp) has been indicated in several points of this figure. Refinement due to the intragranular nucleation of ferrite would be measured between a precipitated volume of 5% and 95%, i.e. from the Ps curve in the RPTT diagram up to approximately the Pf curve.

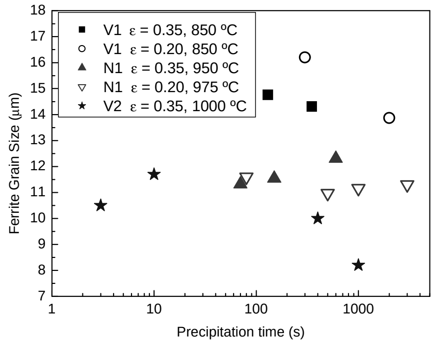

Figure 4. Variation in the ferrite grain size after cooling with the post-deformation isothermal holding time t.

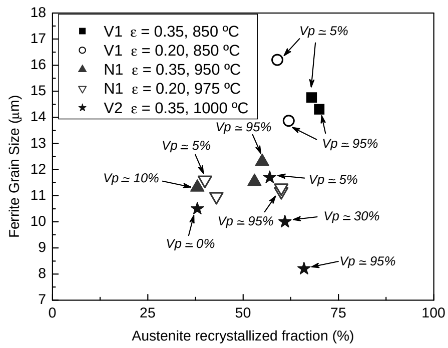

Figure 5. Variation in the ferrite grain size after cooling with the recrystallized fraction. The value of precipitated volume fraction (Vp) is indicated for several points.

From figures 4 and 5, it can be concluded that V-steels V1 and V2 show a decrease in grain size during the time comprised between Ps and Pf curves. This refinement should be mostly attributed to an intragranular nucleation of ferrite on precipitates, as the rest of variables such as the percentage of austenite recrystallization and the grain size remain roughly constant during the duration time of the plateaus [14,15]. In steel V1, the refinement is stronger for the case of lower strains applied, as seen in table 4. In steel N1, a slight decrease in grain size is observed for ε = 0.20, while a coarser ferrite grain size is observed after cooling from Pf when a larger strain (ε = 0.35) is applied. It was previously mentioned that the grain size of steel N1 is finer than the grain of steel V1. The main difference between steels V1 and N1 is the microalloying element. Recrystallization is more sluggish in Nb steels than for V-steels [16]. Consequently, the austenite can start phase transformation with a more strengthened microstructure (higher dislocation density, more elongated grains) that provides a higher density of nucleation sites for ferrite. This can explain the finer ferrite grain size of the samples of steel N1 compared to steel V1. Besides, figures 4 and 5 let to conclude that the intragranular nucleation of ferrite on Nb precipitates is not significant in this steel, as the value of ferrite grain size remains practically constant with holding time. On the other hand, steel V2 presents a more remarkable ferrite grain refinement due to precipitation compared to V1. In steel V2, ferrite grain size is reduced by almost 30% when the sample is cooled after a holding time corresponding to the end of precipitation. The higher amount of C, N and V will certainly cause a different distribution of VCN precipitates that presumably is more favourable for intragranular nucleation than for the case of steel V1 [3,17].

Table 4. Ferrite grain size refinement obtained after cooling from the end of precipitation (Pf, i.e. Vp ≈ 95%) compared to cooling from Ps (Vp ≈ 5%).

Steel	Ferrite grain size refinement obtained after cooling from Pf (compared to cooling from Ps)	
	ε = 0.20	ε = 0.35
V1	-14.4%	-3.0%
N1	-2.6%	+8.8% (increase)
V2	---	-29.9%

3.3. Hot rolling simulation and intragranular nucleation

The above work was carried out in isothermal conditions. In order to study the possible intragranular nucleation in continuous cooling conditions, thermomechanical simulations were carried out by multipass torsion tests on samples of steel V2. These torsion tests let to plot Mean Flow Stress (MFS) curves as that shown in figure 6. The methodology of these tests as well as the way to determine the hot rolling critical temperatures (T_{nr}, A_{r3}, A_{r1}) and the accumulated stress ($\Delta\sigma$) on MFS curves can be found elsewhere [12].

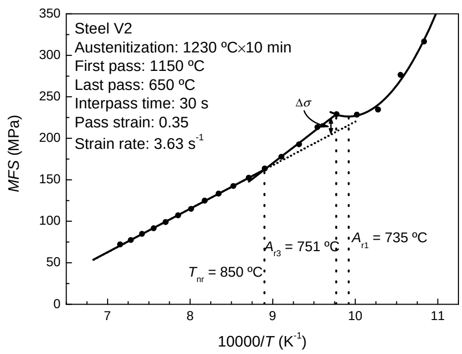

Figure 6. Mean flow stress (MFS) versus the inverse pass temperature measured in a hot rolling simulation by laboratory torsion test. Steel V2. Pass strain = 0.35; interpass time = 30 s.

With the aim of revealing possible intragranular ferrite nucleation on V-precipitates, a microscopy study using FEG-SEM was carried out on several samples tested under hot rolling simulation conditions but performing the last pass at 800ºC and cooling the specimen in an argon stream. Figure 7a shows an example of a SEM image from steel V2 that seems to reveal that V-precipitates can act as nucleation sites for very small ferrite grains near 1 μm size. The mean grain size in this particular sample was close to 4 μm. The observation of several images made it possible to verify the presence of many fine ferritic grains on this specimen and on others tested in different conditions. Peaks corresponding to V, N and C can be found in the spectrum of a VCN particle in figure 7b.

It is known that ferrite grain refinement due to the incomplete recrystallization of austenite is generally weaker in V-microalloyed steels compared to Nb steels, which present a higher value of T_{nr}. However, as shown in figure 8 [18], the phenomenon of intragranular nucleation of ferrite on V particles can contribute to enhance the ferrite grain refinement in hot rolled microalloyed steels.

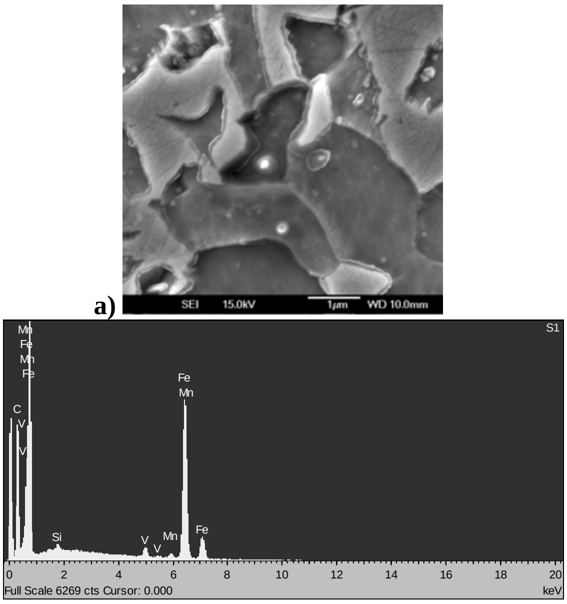

Figure 7. a) SEM image corresponding to a specimen tested in rolling simulation and cooled in argon from 800 ºC. Pass strain = 0.35. Interpass time = 30 s ; **b)** Spectrum of V-carbonitride precipitate of one of the above particles.

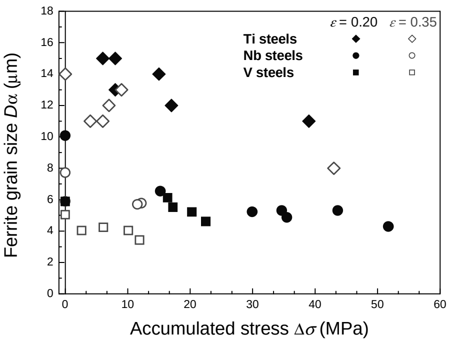

Figure 8. Ferrite grain size as a function of accumulated stress obtained at the end of hot rolling simulations carried out under different conditions of pass strain and interpass time on several low carbon microalloyed steels [18].

4. CONCLUSIONS

- Representation of the ferrite grain size versus the precipitation time and austenite recrystallized fraction, showed an important decrease in the ferrite grain size as the precipitated volume and size increase for V-steels.
- For the same recrystallized fraction, intragranular nucleation was more effective in the steel with a higher content of C, N and V.
- On the other hand, the precipitation state in austenite does not seem to have a remarkable effect on ferrite grain size in the Nb steel studied. Consequently, the intragranular nucleation is not significant in this steel
- Intragranular nucleation of ferrite on V precipitates can contribute to enhance ferrite grain refinement of hot rolled V-microalloyed steels.

5. REFERENCES

[1] J. Yang, K. Zhu, R. Wang, J. Shen: Improving the toughness of heat affected zone of steel plate by use of fine inclusion particles, Steel Research International, 82 (2011), 552-556.

[2] D. Zhang, H. Terasaki, Y. I. Komizo: In situ observation of the formation of intragranular acicular ferrite at non-metallic inclusions in C–Mn steel, Acta Materialia, 58 (2010), 1369–1378.

[3] G. Miyamoto, T. Shinyoshi, J. Yamaguchi, T. Furuhara, T. Maki, U. Uemori: Crystallography of intragranular ferrite formed on (MnS + V(C, N)) complex precipitate in austenite, Scripta Materialia, 48 (2003), 371-377.

[4] D. Glisic, N. Radovic, A. Koprivica, A. Fadel, D. Drobnjak: Influence of Reheating Temperature and Vanadium Content on Transformation Behavior and Mechanical Properties of Medium Carbon Forging Steels, ISIJ International, 50 (2010), 601-606.

[5] X. Li, X. Wang, X. Feng: Effect of Nanophase on the Nucleation of Intragranular Ferrite in Microalloyed Steel, Journal of Wuhan University of Technology-Mater. Sci. Ed., 25 (2010), 228-233.

[6] C. Capdevila, C. Garcia-Mateo, J. Cornide, J. Chao, F.G. Caballero: Effect of V Precipitation on Continuously Cooled Sulfur-Lean Vanadium-Alloyed Steels for Long Products Applications, Metallurgical and Materials Transactions A, 42 (2011), 3743-3751.

[7] J.S. Byun, J.H. Shim, Y.W. Cho, D.N. Lee: Non-metallic inclusion and intragranular nucleation of ferrite in Ti-killed C–Mn steel, Acta Materialia, 51 (2003), 1593-1606.

[8] I. Madariaga, I. Gutiérrez: Role of the Particle-Matrix Interface on the Nucleation of Acicular Ferrite in a Medium Carbon Microalloyed Steel, Acta Materialia, 47 (1999), 951-960.

[9] J.H. Shim, Y.J. Oh, J.Y. Such, Y.W. Cho, J.D. Shim, J.S. Byun, D.N. Lee: Ferrite Nucleation Potency of Non-Metallic Inclusions in Medium Carbon Steels, Acta Materialia, 49 (2001), 2115-2122.

[10] T. Furuhara, J. Yamaguchi, N. Sugita, G. Miyamoto, T. Maki: Nucleation of Proeutectoid Ferrite on Complex Precipitates in Austenite, ISIJ International, 43 (2003), 1630-1639.

[11] E.T. Turkdogan: Causes and Effects of Nitride and Carbonitride Precipitation During Continuous Casting, Iron & Steelmaker, 16 (1989), 61-75.

[12] M. Gómez, L. Rancel, S.F. Medina: Assessment of Austenite Static Recrystallization and Grain Size Evolution during Multipass Hot Rolling of a Niobium-Microalloyed Steel, Metals and Materials International, 15 (2009), 689-699.

[13] S.F. Medina A. Quispe and M. Gómez: Model for static recrystallisation critical temperature in microalloyed steels, Materials Science and Technology, 17 (2001), 536-544.

[14] S.F. Medina, M. Gomez, L. Rancel: Grain refinement by intragranular nucleation of ferrite in a high nitrogen content vanadium microalloyed steel, Scripta Materialia, 58 (2008), 1110-1113.

[15] H.B. Li, H.Y. Liu, Y. Huang: Microstructure refinement in nonquenched and tempered vanadium-nitrogen steel, Advanced Materials Research, 295-297 (2011), 991-996.

[16] S.F. Medina A. Quispe and M. Gómez: Strain induced precipitation effect on austenite static recrystallisation in microalloyed steels, Materials Science and Technology, 19 (2003), 99-108.

[17] J. Ma, X. Zhang, Y. Guan, Z. Deng: Influence of carbon content on the microstructure and precipitates of the V-N microalloyed steels, Advanced Materials Research, 335-336 (2011), 645-649.

[18] M. Gómez, S.F. Medina: Role of microalloying elements in the microstructure of hot rolled steels, International Journal of Materials Research, 102 (2011), 1197-1207.